ANTICANCER RESEARCH *38*: 779-786 (2018)
doi:10.21873/anticanres.12284

Intense Pulsed Light: Friend or Foe? Molecular Evidence to Clarify Doubts

LILIANA FERREIRA[1], RUI VITORINO[2,3], MARIA JOÃO NEUPARTH[4], DAVID RODRIGUES[5], ADELINA GAMA[5,6], ANA I. FAUSTINO-ROCHA[7,8], RITA FERREIRA[1] and PAULA A. OLIVEIRA[5,7]

[1]*Organic Chemistry, Natural Products and Foodstuffs (QOPNA), Mass Spectrometry Center, University of Aveiro, Aveiro, Portugal;*
[2]*Institute for Research in Biomedicine (iBiMED), Department of Medical Sciences, University of Aveiro, Aveiro, Portugal;*
[3]*Cardiovascular Research Unit, Department of Surgery and Physiology, Faculty of Medicine, University of Porto, Porto, Portugal;*
[4]*Research Centre in Physical Activity, Health and Leisure (CIAFEL), Faculty of Sports, University of Porto, Porto, Portugal;*
[5]*Department of Veterinary Sciences, School of Agrarian and Veterinary Sciences, University of Trás-os-Montes and Alto Douro, Vila Real, Portugal;*
[6]*Animal and Veterinary Research Center (CECAV), University of Trás-os-Montes and Alto Douro, Vila Real, Portugal;*
[7]*Center for the Research and Technology of Agro-Environmental and Biological Sciences (CITAB), University of Trás-os-Montes and Alto Douro, Vila Real, Portugal;*
[8]*Faculty of Veterinary Medicine, Lusophone University of Humanities and Technologies, Lisbon, Portugal*

Abstract. *Background/Aim: Intense pulsed light (IPL) has been extensively applied in the field of dermatology and aesthetics; however, the long-term consequences of its use are poorly unknown, and to the best of our knowledge there is no study on the effect of IPL in neoplastic lesions. In order to better understand the molecular mechanisms underlying IPL application in the skin, we used an animal model of carcinogenesis obtained by chemical induction with 12-dimethylbenz(a)anthracene (DMBA) and 12-O-tetradecanoylphorbol-13-acetate (TPA). Materials and Methods: Institute of Cancer Research (ICR) mice were administered DMBA and/or TPA and treated with IPL. Skin was evaluated by histopathology and 2DE-blot-MS/MS analysis. Results: Our data evidenced an inflammatory response and a metabolic remodeling of skin towards a glycolytic phenotype after chronic exposure to IPL, which was accomplished by increased oxidative stress and susceptibility to apoptosis. These alterations induced by IPL were more notorious in the DMBA sensitized skin. Keratins and metabolic proteins seem to be the more susceptible to oxidative modifications that might result in loss of function, contributing for the histological changes observed in treated skin. Conclusion: Data highlight the deleterious impact of IPL on skin phenotype, which justifies the need for more experimental studies in order to increase our understanding of the IPL long-term safety.*

Correspondence to: Ana I. Faustino, CITAB, Faculty of Veterinary Medicine, Lusophone University of Humanities and Technologies, Lisbon, Portugal. Tel: +351 968914559, e-mail: anafaustino.faustino@sapo.pt

Key Words: Mice, carcinogenesis, blot-MS/MS, oxidative stress, 2-DE.

Skin cancer is a global public health problem that affects every ethnic, socio-economic and demographic groups. The incidence of this type of cancer has increased in the recent decades. Basal cell carcinoma (BCC) is the most common type of skin cancer worldwide and although the mortality rate is low, it has a significant morbidity associated with economic impact to health services (1).

Intense Pulsed Light (IPL) has been extensively used in dermatology for the treatment of several vascular conditions and even for purely aesthetic reasons. Among the principal dermatological applications of this type of radiation are telangiectasias, irregular pigmentation, hair removal, and photorejuvenation (2, 3). IPL is a type of non-laser radiation comprising high intensity wavelengths in the range of 515-1200 nm (2, 4). These devices are configured for a fixed duration of light pulse and do not require training in their use, being accessible to every person (5). Nevertheless, negative

side effects of IPL application were reported such as pain, inflammation, edema and the formation of crusts with possible occurrence of infections and scarring (2, 6). Cutaneous hyperpigmentation or hypopigmentation might also occur, resulting in permanent damage of melanocytes (4).

Despite the intensive use of IPL and the clinical dermatological benefits reported, few studies have explored the molecular mechanisms activated by this radiation in skin that help to preclude the long-term effects of skin exposition to IPL, and none has evaluated the impact of IPL in skin pre-neoplastic lesions. In order to give new insights on IPL-induced molecular pathways in healthy skin and with pre-malignant lesions, we used an animal model of skin carcinogenesis daily exposed to IPL for 25 weeks. Using 2DE-blot-MS/MS of skin extracts we identified the proteins more susceptible to oxidative modifications and the potential signaling pathways involved, which were further related to the histological alterations promoted by IPL.

Materials and Methods

Animal protocol. Twenty-eight female mice (Mus musculus, ICR (CD-1®)) with 5 weeks old were obtained from Harlan Interfauna (Barcelona, Spain). After 1 week of acclimatization, the animals were randomly divided into five experimental groups: Control (n=5); DMBA (n=5); DMBA+TPA (n=6); DMBA+IPL (n=6); IPL (n=6). Animals were housed in plastic cages, with hard wood chips for bedding, and maintained on a basal diet (4RF21®, Mucedola, Settimo Milanese, Milan, Italy). The room temperature and the relative humidity were controlled at 23±2˚C and 50±10%, respectively. The following protocol was approved by the Portuguese Ethics Committee for Animal Experimentation and was performed in accordance to the National and European Community Legislation for Animal Welfare (National Decree-Law 113/2013 and European Directive 2010/63/EU).

Animal protocol was initiated with the hair cutting of the mice dorsum region to be exposed to chemical agents and/or IPL. The hair cut was made with a shearing machine (Aesculap GT420 Isis, Aesculap Inc., Center Valley, PA, USA). In the animals from groups DMBA, DMBA+IPL and DMBA+TPA, it was topically applied a single dose of the initiator agent 12-dimethylbenz(a)anthracene (DMBA, 2 mM prepared in acetone). Four days after the application of DMBA, 12-O-tetradecanoylphorbol-13-acetate (TPA, 100 mM prepared in acetone) was applied to the animals from DMBA+TPA group twice a week for 25 weeks. The animals from groups DMBA+IPL and IPL were exposed to intense pulsed light (Lumea SC2001/00, Phillips, Amsterdam, Netherlands), 2 pulses at an intensity of 5, which correspond to 6.5 J/cm^2 in an area of 6 cm^2, twice a week and throughout the animal protocol. IPL pulses were applied parallel to the sagittal line of the mice. Acetone was topically applied, twice a week, to the skin of the animals from control group. Animals were observed daily for health check.

At the end of the experimental protocol, animals were euthanized with ketamine/xylazine (Imalgene® 1000, Merial S.A.S., Lyon, France and Rompun® 2%, Bayer Healthcare S.A., Kiel, Germany, respectively) and blood was collected. All noticeable tumors in the skin region submitted to the tested treatments were counted and removed for biochemical and histologic analysis.

Skin histologic analysis. Cubic pieces from skin tissue were fixed [4% (v/v) buffered paraformaldehyde] by diffusion during 24 h and subsequently dehydrated with graded ethanol and included in paraffin blocks. Serial sections (2 μm of thickness) of paraffin blocks were cut by a microtome (Leica®20035, Leica Microsystems, Wetzlar, Germany). Deparaffinized sections of skin tissue were stained for hematoxylin-eosin and classified according to Thomas-Ahner 2007 (7).

Blood tests. Serum albumin, total protein, the activity the alanine aminotransferase (ALT) and aspartate aminotransferase (AST) were measured in duplicate on an AutoAnalyzer (Prestige 24i, Cormay PZ, Diamond Diagnostics, Holliston, MA, USA). Serum C-reactive protein and IL-6 levels were assayed by immunoblotting as described below.

Preparation of skin samples for biochemical analysis. Skin specimens homogenized in solubilization buffer (7 M urea, 2 M thiourea, 4% CHAPS, 0.1% PMSF) in the ratio of 50 mg tissue per ml of solubilization buffer. The homogenization was performed with a Potter-Elvehjem homogenizer and a Teflon pestle. All the procedures were performed on ice or below 4˚C. Protein content was determinate with the RD DC Protein Assay Kit (Bio-Rad, Holliston, CA, USA).

Immunoblotting analysis. For the analysis of CRP and IL-6, serum samples were diluted 1:20 in TBS and a volume of 100 μl was slot-blotted into a nitrocellulose membrane. For the analysis of metabolic proteins, equivalent amounts of skin tissue proteins of each group were electrophoresed on a 12.5% SDS-PAGE. Gels were blotted onto a nitrocellulose membrane (Whatman®, Protan®) in transfer buffer (25 mM Tris, 192 mM glycine and 20% methanol) during 2 h (200 mA). For the analysis of 3-nitrotyrosine, skin extracts were diluted in TBS to obtain a final protein concentration of 0.001 μg/μl and a volume of 100 μl was slot-blotted into a nitrocellulose membrane. Then, nonspecific binding was blocked with 5% (w/v) dry nonfat milk in TBS-T (100 mM Tris, 1.5 mM NaCl, pH 8.0 and 0.5% Tween 20). Membranes with serum samples were incubated with primary antibody diluted 1:1000 5% (w/v) nonfat dry milk in TBS-T (anti-C-reactive protein (CRP; ab32412, Abcam, Cambridge, UK) or anti-Interleukin-6 (IL-6; ab6672, Abcam, Cambridge, UK)) for 2 h at room temperature, washed and incubated with secondary horseradish peroxidase-conjugated anti-rabbit (1:1,000; GE Healthcare, Milwaukee, WI, USA). Membranes with skin extracts were incubated with primary antibody diluted 1:1000 in 5% (w/v) non-fat dry milk in TBS-T (anti-GAPDH (ab9485, Abcam, Cambridge, UK), anti-ATP synthase subunit β (ab14730, Abcam, Cambridge, UK), anti-p53 (Sc99, Santa Cruz, Dallas, Tx, USA), anti-cleaved caspase-3 (PC679, CalbioChem, San Diego, CA, USA), anti-3-nitrotyrosine (06-284, Merck Millipore, Darmstadt, Germany)) for 2 h at room temperature, washed and incubated with secondary horseradish peroxidase-conjugated anti-rabbit (GE Healthcare, Milwaukee, WI, USA), respectively. Immunoreactive bands were detected by enhanced chemiluminescence ECL (Amersham Pharmacia Biotech, Piscataway, NJ, USA) according to the manufacturer's procedure and images were recorded using X-ray films (Kodak Biomax Light Film, Sigma, MO, USA). The films were scanned in Molecular Imager Gel Doc XR+ System and analyzed with QuantityOne software (v4.1, Bio-Rad, Holliston, CA, USA). Control for protein loading was confirmed by Ponceau S staining.

For the protein carbonyl derivate assay, a given volume (V) of sample containing 20 μg of protein was derivatized with 2,4-dinitrophenylhydrazine (DNPH). Briefly, the sample was mixed with

Table I. *Biochemical parameters analyzed in the serum of the animals from the different experimental groups. Values are expressed as mean±standard deviation of concentration or activity.*

Group	Total Protein (g/L)	Albumin (g/L)	Alanine aminotransferase (ALT) (U/L)	Aspartate aminotransferase (AST) (U/L)
DMBA	54.57±0.90##	33.42±0.80###	39.68±4.11	169.50± 40,63**###
DMBA+IPL	48.23±4.19***	29.33±2.40**	32.53±2.47##	180.60±66.23#
DMBA+TPA	49.82±2.69*	29.18±0.43**	47.12±14.22*	138.10±8.22
IPL	52.40±1.79	31.27±1.47#	42.40±3.63	150.60±45.81
Control	54.38±3.81	32.03±2.31	36.26±4.79	129.70±16.14

*$p<0.05$ *vs*. control; **$p<0.01$ *vs*. control; ***$p<0.001$ *vs*. control; #$p<0.05$ *vs*. DMBA+TPA; ##$p<0.01$ *vs*. DMBA+TPA; ###$p<0.001$ *vs*. DMBA+TPA.

1V of 12% sodium dodecyl sulfate, 2V of 2 mM DNPH/10% trifluoroacetic acid, followed by 30 minutes of incubation in the dark, after which 1.5 V of 2 M Tris-base/18.3% of β-mercaptoethanol was added for neutralization. After diluting the derivatized proteins in TBS to obtain a final concentration of 0.001 μg/μl, a 100 μl volume was slot-blotted into a nitrocellulose membrane. Immunodetection was performed as above-referred with anti-DNP (1:1000, V041, DakoCytomation, Glostrup, Denmark) as primary antibody.

2DE-blot-MS/MS analysis. In brief, 150 μg proteins of skin extracts were diluted to 125 μl with a rehydration solution containing 8 M urea, 2 M thiourea, 1% CHAPS, 12.9 mM DTT, 1% ampholytes 3-10; 0.01% of blue bromophenol and loaded on 7 cm IPG strips (pH 3-10 NL; GE Healthcare, Milwaukee, WI, USA) with a pH 3-10. The isoelectric separation was performed using the following focusing program: 12 h at 50 mV in rehydration, 2 h at 150 V (gradient), 1 h at 500 V (gradient), 1 h at 1,000 V (gradient) and 1.5 h at 5,000V ("step-n-hold"). After IEF separation, the gel strips were applied on top of a 12.5% SDS-PAGE and proteins were separated at 150 V constant current until the bromophenol blue front reached the bottom of the gel. Gels were stained with BlueSafe (Nztech) or were blotted onto a nitrocellulose membrane (Whatman®, Protan®) in transfer buffer (25 mM Tris, 192 mM glycine and 20% methanol) during 2 h (200 mA).

For the analysis of carbonylated proteins, before SDS-PAGE, strips were incubated with 5 ml of 12% SDS, during 20 min, followed by incubation with 5 ml of 20 mM DNPH solution, during 1 h in the dark with agitation. Then, strips were incubated for 30 min with a solution buffer containing 2% (w/v) SDS, 6 M urea, 30% glycerol, 0.05 M Tris-HCl pH 8,8 and 20 mg/ml DTT.

Immunodetection of carbonylated and nitrated proteins was performed as above described. Gels and films were scanned into the Gel Doc XR + System (Bio-Rad, Holliston, CA, USA) and analyzed using PDQuest software (v7.2, Bio-Rad, Holliston, CA, USA).

The protein spots immunostained with anti-DNP or with anti-3-nitrotyrosine were removed from the 2D-gel, destained with 25 mM ammonium bicarbonate/50% acetonitrile, and dried in vacuum concentrator (SpeedVac, Thermo Savant). The dried gel pieces were rehydrated with 25 μl of 10 μg/ml trypsin in 50 mM ammonium bicarbonate and digested overnight at 37˚C. Tryptic peptides were dried in a vacuum concentrator and resuspended in 10 μl of a 50% acetonitrile/0.1% formic acid solution. MS was performed on a matrix-assisted laser desorption/ionization-time-of-flight MALDI-TOF/TOF mass spectrometer (4800 Proteomics Analyzer, AbSCIEX) in the positive ion reflector mode. The ten most intense peaks in each spot were selected for further perform of MS/MS spectra, excluding the peaks of trypsin autolysis or of acrylamide. The spectra were processed and analyzed by Global Protein Server Workstation (Applied Biosystems, Foster City, CA, USA), which uses as Mascot search engine (Matrix Science, London, UK), for the identification of proteins, combining data from PMF (peptide mass fingerprinting) with MS/MS data for research in an internal database. The protein identification was considered when the degree of confidence was higher than 98%.

Statistical analysis. The variables analyzed showed a normal distribution, according to the Kolmogorov-Smirnov test. For this reason, the results obtained from biochemical analyses were processed using parametric statistical tests. Differences between experimental groups were analyzed by one-way ANOVA followed by Tukey *post-hoc* test for multiple comparisons. The calculations were performed with the software GraphPad Prism (version 5.0, La Jolla, CA, USA). The values obtained were considered statistically significant when $p<0.05$. The results for all variables are presented as mean±standard deviation.

Results

Characterization of animals' response to treatments. At the end of the experimental protocol, animals treated with the initiation and promotor carcinogenic agents (DMBA+TPA group) showed a lower gain of body weight ($p<0.05$ *vs*. control; data not shown). Serum analysis also evidenced significant lower levels of serum albumin and total protein ($p<0.01$ and $p<0.05$ *vs*. control, respectively, Table I), and significantly higher levels of the inflammatory markers Interleukin-6 (IL-6) and C-reactive protein (CRP) ($p<0.001$ *vs*. control, Figure 1). Though DMBA+TPA was the group that showed the highest values of these serum markers of inflammation, the other experimental groups also presented significant increased levels of CRP and IL-6 compared to control (Figure 1). The activity of serum alanine transaminase (ALT) in DMBA+TPA was higher than in control group ($p<0.01$, Table I). Application of DMBA and DMBA combined with IPL promoted an increased activity of serum aspartate transaminase (AST; $p<0.01$ and $p<0.05$ *vs*. control, respectively, Table I).

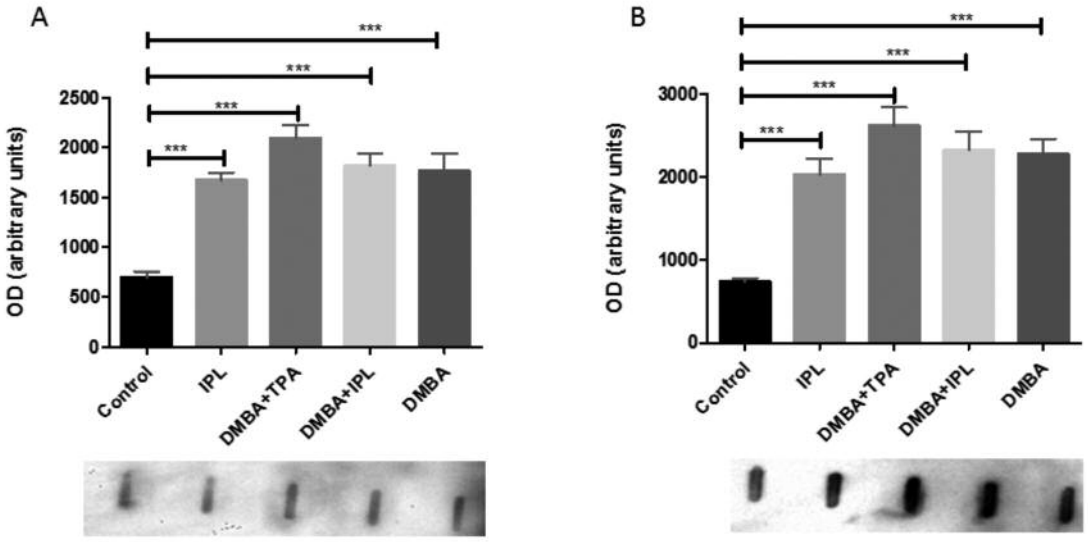

Figure 1. *Interleukin-6 (A) and C-reactive protein (B) levels evaluated by immunoblotting in the serum of animals from the different experimental groups. Representative immunoblots are presented below the respective graphs. The values of the optical density (OD) are expressed in arbitrary units. ***p<0.001 vs. control.*

Histological and biochemical changes induced by treatments. During the experimental protocol, changes in the skin of animals from group DMBA+TPA were noticed, such as flaking skin regions. Histological analysis confirmed the presence of skin neoplastic lesions in this group of animals. Three mice had squamous cell carcinoma, associated with the presence of inflammatory infiltrate. Animals from DMBA group presented a negligible and diffuse inflammatory infiltrate, while animals from DMBA+IPL group showed focal hyperplasia and inflammatory infiltrate in the dermis, although less significant than the observed in the DMBA+TPA group.

In order to evaluate the biological processes underlying these histological changes, we measured the expression of the metabolic proteins ATP synthase subunit β and glyceraldehyde 3-phosphate dehydrogenase (GAPDH) by western blotting. Data showed a significant increase in the levels of ATP synthase, in all groups of animals treated with DMBA ($p<0.001$ DMBA+TPA *vs.* control, DMBA+IPL *vs.* control; $p<0.01$ DMBA *vs.* control, Figure 2A). Regarding IPL group, no statistical significant differences were noticed in comparison to the control. The expression of ATP synthase subunit β in DMBA+TPA group was significantly different from all other groups ($p<0.001$). The levels of the glycolytic enzyme GAPDH were also significantly higher in skin extracts from all experimental groups when compared to the control group (Figure 2B). DMBA+TPA and DMBA+IPL groups showed similar values among them and significantly higher compared to IPL and DMBA groups ($p<0.05$, Figure 2B). The analysis of the ratio ATP synthase/GAPDH suggests that DMBA and/or IPL promoted the metabolic remodeling of the skin towards a glycolytic phenotype (Figure 2C). These metabolic changes were related to an increased susceptibility to apoptosis. Indeed, higher expression levels of p53 and cleaved caspase-3 were noticed in the skin of animals from DMBA+TPA and DMBA+IPL groups ($p<0.001$ and $p<0.05$ *vs.* control, respectively for p53 (Figure 2D) and $p<0.001$ *vs.* control for cleaved caspase-3 (Figure 2E)). Still, all the treatments tested promoted an increase of cleaved caspase-3 levels.

Skin metabolic remodeling was paralleled by increased oxidative stress, given by augmented content of carbonylated and/or nitrated proteins. Indeed, the levels of carbonylated proteins were significantly higher in the skin extracts of IPL and DMBA+IPL groups, compared to control ($p<0.05$ and $p<0.001$, respectively). Curiously, no differences were noticed in the levels of carbonylated proteins in DMBA+TPA compared to control group (Figure 3B), which seems to be justified by the significantly higher content of nitrated proteins ($p<0.001$ all groups *vs.* DMBA+TPA, Figure 4A). These results suggest that DMBA+TPA treatment led to an increased generation of nitric oxide ($NO^{\bullet}$) that reacted with superoxide anion ($O2^{\bullet-}$) with the formation of peroxynitrite ($ONOO^{-}$). This chemical specie then reacted with skin proteins' tyrosine residues (7). The levels of nitrated proteins in DMBA + IPL group were also significantly higher compared to the control group ($p<0.01$, Figure 3A).

In order to identify the proteins more susceptible to oxidative damage, 2DE-blot followed by MS/MS analysis was performed. The 2DE profiles of carbonylated proteins were similar among DMBA and DMBA+IPL groups, but differed

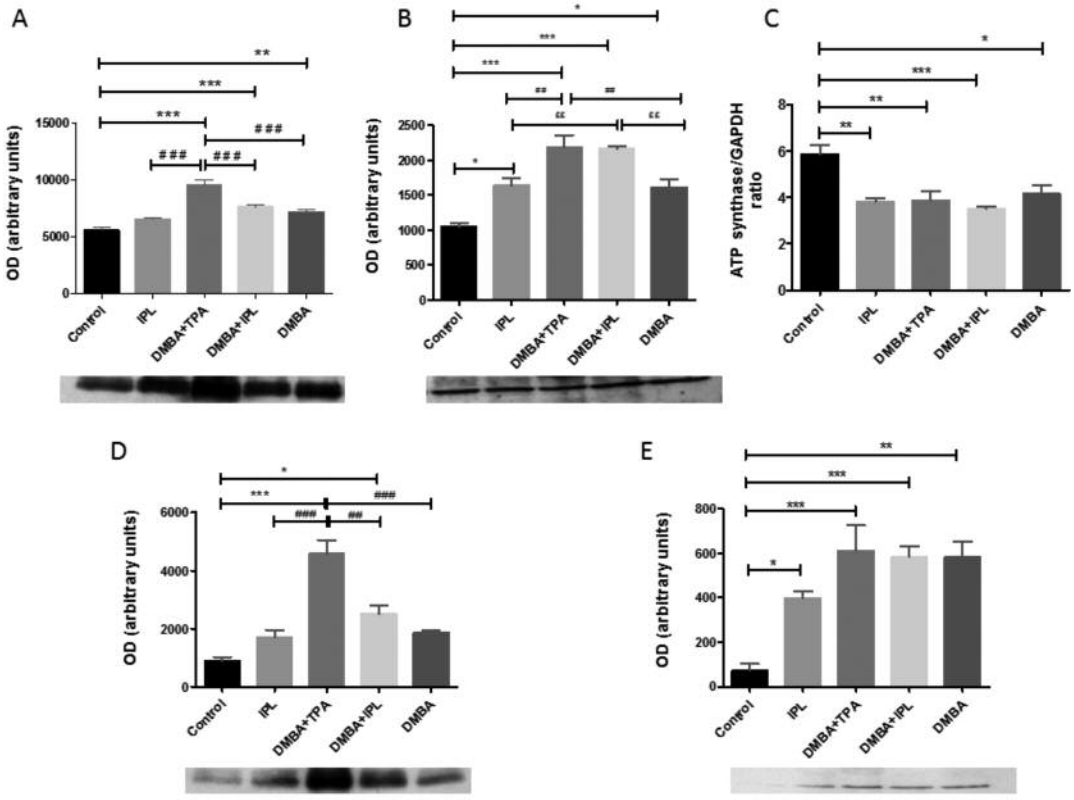

Figure 2. *ATP synthase β subunit (A), GAPDH (B), p53 (D) and cleaved caspase-3 (E) evaluated by western blotting in skin extracts from mice of all experimental groups. Representative images of immunoblots are shown below the respective graphs. In (C) the ratio ATP synthase/GAPDH is presented. Optical density values are expressed in arbitrary units. *p<0.05 vs. control; **p<0.01 vs. control; ***p<0.001 vs. control; ##p<0.01 vs. DMBA+TPA; ###p<0.001 vs. DMBA+TPA; ££p<0.01 vs. DMBA+IPL.*

from the ones of nitrated proteins. In general, nitrated proteins presented pI 4-6 and lower molecular weight, 30-40 kDa than carbonylated ones (Figure 4). The spots corresponding to the oxidized proteins (nitrated and carbonylated) were excised from the 2-DE gels for further analysis by MS/MS and the identified proteins are listed in Table II. Among the proteins more susceptible to oxidation, different isoforms of keratin, α-actin, cytoplasmic actin 1 and β-actin of type 2 were identified. These proteins are part of the intermediate filaments and of microfilaments of the cytoskeleton. Regarding keratin cytoskeletal isoforms, type I (10 and 17 isoforms) and type II (isoforms 6A and 6B) were identified. These types of keratin are often designated as cytokeratins and were found carbonylated in DMBA+IPL and DMBA+TPA groups. Protein-protein interaction analysis performed with the bioinformatics tool String 9.1 considering the proteins found carbonylated highlighted the interaction with profilins (Pfn1 and Pfn2), fibronectin (Fn1), VEGF (Vegfa) and kininogen 1 (Kng1). Among the proteins more susceptible to nitration, metabolic proteins as enolase and GAPDH, and proteins involved in apoptosis, such as galectin-7 and casein kinase were identified (Table II). Protein-protein interaction analysis performed with the String 9.1 considering the proteins found nitrated highlighted metabolism as the biological process more prone to regulation by this type of oxidative modification (data not shown).

Discussion

IPL has been extensively applied in the field of dermatology and aesthetics, for the treatment of irregular pigmentation, vascular lesions, in the removal of hair and in photo-rejuvenation (2, 3, 8, 9). However, the long-term consequences of the use of this type of radiation are poorly unknown, and to the best of our knowledge there is no study on the effect of IPL in neoplastic lesions. So, aiming to better understand the molecular mechanisms underlying IPL application in the skin, we used an animal model of carcinogenesis obtained by chemical induction with DMBA and TPA (10, 11).

DMBA at low concentrations is known to activate the oncogene *H-ras* in the epithelial cells of the skin. The repeated application of TPA promotes the development of skin lesions,

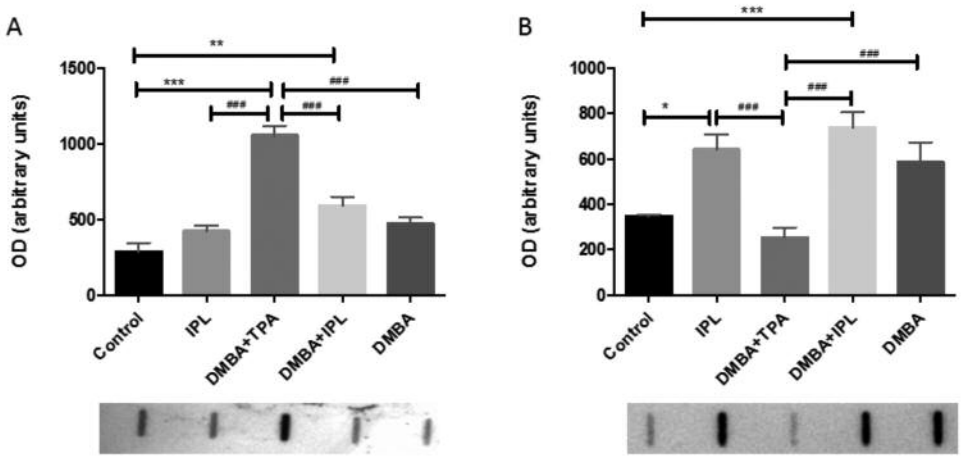

Figure 3. *Total content of nitrated (A) and carbonylated (B) proteins estimated by immunoblotting in mice skin extracts from all experimental groups. Representative images of immunoblots are presented below the respective graphs. The optical density values are expressed in arbitrary units. *p<0.05 vs. control; **p<0.01 vs. control; ***p<0.001 vs. control; ###p<0.001 vs. DMBA+TPA.*

which can progress to squamous cell carcinoma (11), the most aggressive and lethal non-melanoma skin cancer (12). The histological analysis of skin sections supported the efficiency of DMBA combined with TPA in the induction of neoplastic lesions, once five out of six animals exposed to DMBA and TPA showed skin papillomas and three presented squamous cell carcinoma. The significant higher serum levels of CRP and IL-6 support the inflammatory phenotype associated with skin lesions, which might justify the lower body weight gain observed in these animals. Pro-inflammatory cytokines may induce skeletal muscle loss as previously suggested using the same animal model of carcinogenesis. Moreover, IL-6 levels were previously correlated with malignant squamous cell carcinoma (13, 14) and high plasma levels of CRP were associated with the risk of several types of cancer, including non-melanoma skin cancer (15).

Exposure to IPL also promoted a systemic inflammatory response in mice given by increased serum levels of IL-6 and CRP as well as decreased serum levels of albumin. This inflammatory phenotype was not accomplished by macroscopic alterations suggestive of skin injury. At a molecular level, chronic exposure to IPL induced a metabolic switch in the skin towards glycolysis, which was accomplished by increased oxidative stress given by augmentation of carbonylated proteins. Increased generation of ROS are expected to damage protein complexes and enzymes, as well as membranes and DNA, impairing the oxidative phosphorylation ability to synthetize ATP (16). These results suggest that skin cells respond to IPL in a similar way as reported for UV radiation. Lenz *et al.* (17) verified that skin cells compensate the loss of mitochondrial energetic capacity by extra-mitochondrial pathways such as glycolysis. The UV-induced metabolic switch to catabolic pathways for ATP generation seems to be mediated by the

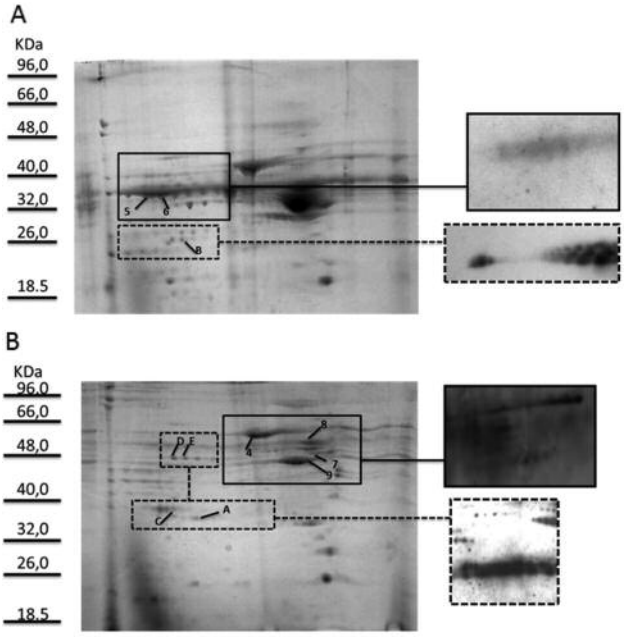

Figure 4. *Representative 2-DE profile for DMBA+TPA (A) and DMBA+IPL (B) groups showing the gel spots reactive to anti-DNP (solid line boxes) and to anti-3-nitrotyrosine (dotted boxes) antibodies. The numbers and letters have correspondence to Table II.*

activation of AMPK, which positively regulates downstream p53 activation (18) Our data supports p53 activation induced by IPL, which impacted skin cells apoptosis given by the increased levels of cleaved caspase-3. The overexpression of epidermal p53 was previously reported in patients with Fitzpatrick skin type III to IV after IPL treatment, and was related to dysregulation of apoptosis and increased risk of skin cancer (19).

Table II. *List of proteins identified by MS/MS in 2-DE reactive spots to anti-DNP (identified by numbers) and to anti-3-nitrotyrosine (identified by letters) antibodies.*

Spot	Protein name	Uiprot accession number	Accession number	Gene	Score	Protein MW (Da)	pI	Peptide count
1	Actin alpha	P68134	ACTS_MOUSE	*Acta1*	208	42023.9	5.23	13
2	Beta-actin-like protein 2	Q8BFZ3	ACTBL_MOUSE	*Actbl2*	48	41977.0	5.30	1
3	Small conductance calcium-activated potassium channel protein 2	P58390	KCNN2_MOUSE	*Kcnn2*	39	63441.8	9.58	1
4	Serum albumin	P07724	ALBU_MOUSE	*Alb*	160	68647.7	5.75	10
5	Keratin type II cytoskeletal 6B	Q9Z331	K2C6B_MOUSE	*Krt6b*	209	60285.1	8.51	13
6	Keratin type II cytoskeletal 6A	P50446	K2C6A_MOUSE	*Krt6a*	144	59298.6	8.04	11
7	Keratin type I cytoskeletal 17	Q9QWL7	K1C17_MOUSE	*Krt17*	164	60285.1	5.00	19
8	Keratin type I cytoskeletal 10	P02535	K1C10_MOUSE	*Krt10*	133	57735.1	5.04	13
9	Actin cytoplasmic 1	P60710	ACTB_MOUSE	*Actb*	107	41709.7	5.29	3
A	Carbonic anhydrase 3	P16015	CAH3_MOUSE	*Ca3*	95	29347.6	6.89	5
B	Glyceraldehyde-3-phosphate dehydrogenase	P16858	G3P_MOUSE	*Gapdh*	67.2	35787.2	8.44	4
C	Creatine kinase M-type	P07310	KCRM_MOUSE	*Ckm*	56.11	43017.8	6.58	1
D	Beta-enolase	P21550	ENOB_MOUSE	*Eno3*	71.6	46995.3	6.73	5
E	Casein kinase II subunit alpha	O54833	CSK22_MOUSE	*Csnk2a2*	52.9	41189.1	8.64	5
F	Galectin-7	O54974	LEG7_MOUSE	*Lgals7*	81.2	15163.8	6.70	1
G	Transthyretin	P07309	TTHY_MOUSE	*Ttr*	46.8	15766.0	5.77	2

IPL irradiation of skin previously exposed to DMBA induced focal hyperplasia in the dermis with negligible inflammatory infiltrate, as described earlier (11). These histological alterations were related to the metabolic remodeling of skin towards glycolysis and increased oxidative stress, characterized by a significant increase of carbonylated and nitrated proteins. This increase was higher in DMBA+IPL than in IPL group. The formation of carbonyl groups is a common phenomenon under conditions of oxidative stress and results from ROS-induced oxidation of some amino acid residues of protein (20, 21). In the presence of high content of NO, peroxynitrite might be formed and react with proteins (22). Curiously, in the skin of animals exposed to DMBA and TPA no significant alterations of carbonylated protein levels were noticed but the amount of nitrated proteins was significantly higher, approximately 5-fold, than in all other groups. These differences seem to be justified by the significant infiltration of inflammatory cells in the skin of DMBA+TPA animals, with the concomitant increase of NO due to the activity of the inducible nitric oxide synthase (iNOS), which expression is activated by pro-inflammatory cytokines (23). These oxidative changes often lead to function loss, fragmentation, unfolding/misfolding or aggregation of proteins (24). Metabolic proteins as beta-enolase and carbonic anhydrase 3 (CA3) were among the proteins most susceptible to this type of oxidative modification. The presence of CA3 in skin was previously reported and nitration-induced loss of CA3 activity was related to the alkalization of the skin surface (25).

Among the most susceptible proteins to carbonylation, different isoforms of keratin were identified. Keratins are the most abundant proteins of cornea layer and were previously reported to be the skin proteins more susceptible to oxidative modifications promoted by oxidizing agents (*e.g.* UVA, benzoyl-hydroperoxide and hypochlorite) (26). Once carbonylation is often related with protein loss of function (21), we might speculate that the loss of keratins integrity and function might underlie the morphological changes observed in the skin of these groups of animals. Actin filaments are also particularly susceptible to oxidative modifications. Moderate oxidation of actin proteins has a limited effect on the ability of polymerization of these filaments, otherwise carbonylated actin proteins aggregate and become toxic to the cell, if not degraded by proteasome (27, 28). In the present study we noticed a higher susceptibility of α-actin and β-actin of type 2 to carbonylation, particularly in the DMBA+IPL group. The loss of their function is expected to impair the organization of the cytoskeleton, which might trigger skin tumorigenesis (29).

Conclusion

Taken together, our data suggest that chronic exposure to IPL promotes a metabolic remodeling of skin towards a glycolytic phenotype, which is accomplished by increased oxidative stress and susceptibility to apoptosis. These alterations induced by IPL were more notorious in the DMBA sensitized skin. Keratins and metabolic proteins seem to be the more susceptible to oxidative modifications that might result in loss of function, contributing for the histological changes observed in treated skin. Data highlight the deleterious impact of IPL on skin phenotype, which

justifies the need for more experimental studies in order to increase our understanding of the IPL long-term safety.

Conflicts of Interest

There Authors have no conflicts of interest to declare.

Acknowledgements

This work was supported by Portuguese Foundation for Science and Technology (FCT), European Union, QREN, FEDER and COMPETE for funding iBiMED (UID/BIM/04501/2013), UnIC (UID/IC/00051/2013) and QOPNA (UID/QUI/UI0062/2013) research units, RNEM (Rede Nacional de Espectrometria de Massa), the Investigator Grant to RV (IF/00286/2015) and the project grant to PAO (PTDC/DTP-DES/6077/2014).

References

1 Lomas A, Leonardi-Bee J and Bath-Hextall F: A systematic review of worldwide incidence of nonmelanoma skin cancer. Brit J Dermatol *166(5)*: 1069-1080, 2012.
2 Babilas P: Intense pulsed light (IPL): a review. Lasers Surg Med *42(2)*: 93-104, 2010.
3 Raulin C, Greve B and Grema H: IPL technology: a review. Lasers Surg Med *32(2)*: 78-87, 2003.
4 Wat H, Wu DC, Rao J and Goldman MP: Application of intense pulsed light in the treatment of dermatologic disease: a systematic review. Dermatol Surg *40(4)*: 359-377, 2014.
5 Town G and Ash C: Are home-use intense pulsed light (IPL) devices safe? Laser Med Sci *25(6)*: 773-780, 2010.
6 Moreno-Arias GA, Castelo-Branco C and Ferrando J: Side-effects after IPL photodepilation. Dermatol Surg *28(12)*: 1131-1134, 2002.
7 Bickers DR and Athar M: Oxidative stress in the pathogenesis of skin disease. J Invest Dermatol *126(12)*: 2565-2575, 2006.
8 Ciocon, DH, Boker A and Goldberg DJ: Intense pulsed light: what works, what's new, what's next. Facial Plast Surg *25(5)*: 290-300, 2009.
9 Goldberg DJ: Current trends in intense pulsed light. J Clin Aesthet Dermatol *5(6)*: 45-53, 2012.
10 Abel EL, Angel JM, Kiguchi K and DiGiovanni J: Multi-stage chemical carcinogenesis in mouse skin: fundamentals and applications. Nat Protoc *4(9)*: 1350-1362, 2009.
11 Chaudhary SC, Alam MS, Siddiqui MS and Athar M: Chemopreventive effect of farnesol on DMBA/TPA-induced skin tumorigenesis: involvement of inflammation, Ras-ERK pathway and apoptosis. Life Sci *85(5-6)*: 196-205, 2009.
12 Kemp CJ: Multistep skin cancer in mice as a model to study the evolution of cancer cells. Semin Cancer Biol *15(6)*: 460-473, 2005.
13 Lederle W, Depner S, Schnur S, Obermueller E, Catone N, Just A, Fusenig NE and Mueller MM: IL-6 promotes malignant growth of skin SCCs by regulating a network of autocrine and paracrine cytokines. Int J Cancer *128(12)*: 2803-2814, 2011.
14 Taniguchi K and Karin M: IL-6 and related cytokines as the critical lynchpins between inflammation and cancer. Semin Immunol *26(1)*: 54-74, 2014.
15 Trichopoulos D, Psaltopoulou T, Orfanos P, Trichopoulou A and Boffetta P: Plasma C-reactive protein and risk of cancer: a prospective study from Greece. Cancer Epidemiol, Biomarkers and Prev *15(2)*: 381-384, 2006.
16 Vallejo CG, Cruz-Bermúdez A, Clemente P, Hernández-Sierra R, Garesse R and Quintanilla M: Evaluation of mitochondrial function and metabolic reprogramming during tumor progression in a cell model of skin carcinogenesis. Biochim *95(6)*: 1171-1176, 2013.
17 Lenz H, Schmidt M, Welge V, Schlattner U, Wallimann T, Elsässer HP, Wittern KP, Wenck H, Stäb F and Blatt T: The creatine kinase system in human skin: protective effects of creatine against oxidative and UV damage *in vitro* and *in vivo*. J Invest Dermatol *124(2)*: 443-452, 2005.
18 Cao C, Lu S, Kivlin R, Wallin B, Card E, Bagdasarian A, Tamakloe T, Chu WM, Guan KL and Wan Y: AMP-activated protein kinase contributes to UV- and H_2O_2-induced apoptosis in human skin keratinocytes. J Biol Chem *283(43)*: 28897-28908, 2008.
19 El-Domyati M, El-Ammawi TS, Medhat W, Moawad O, Mahoney MG and Uitto J: Expression of p53 protein after nonablative rejuvenation: the other side of the coin. Dermatol Surg *39(6)*: 934-943, 2013.
20 Berlett BS and Stadtman ER: Protein oxidation in aging, disease, and oxidative stress. J Biol Chem *272(33)*: 20313-20316, 1997.
21 Fedorova M, Bollineni RC and Hoffmann R: Protein carbonylation as a major hallmark of oxidative damage: update of analytical strategies. Mass Spectrom Rev *3(2)*: 79-97, 2014.
22 Szabo E, Virág L, Bakondi E, Gyüre L, Haskó G, Bai P, Hunyadi J, Gergely P and Szabó C: Peroxynitrite production, DNA breakage, and poly(ADP-ribose) polymerase activation in a mouse model of oxazolone-induced contact hypersensitivity. J Invest Dermatol *117(1)*: 74-80, 2001.
23 Greenacre SA, Rocha FA, Rawlingson A, Meinerikandathevan S, Poston RN, Ruiz E, Halliwell B and Brain SD: Protein nitration in cutaneous inflammation in the rat: essential role of inducible nitric oxide synthase and polymorphonuclear leukocytes. Brit J Pharmacol *136(7)*: 985-994, 2002.
24 Perluigi M, Di Domenico F, Blarzino C, Foppoli C, Cini C, Giorgi A, Grillo C, De Marco F, Butterfield DA, Schininà ME and Coccia R: Effects of UVB-induced oxidative stress on protein expression and specific protein oxidation in normal human epithelial keratinocytes: a proteomic approach. Proteome Sci *8*: 13, 2010.
25 Kawasaki H, Tominaga M, Shigenaga A, Kamo A, Kamata Y, Iizumi K, Kimura U, Ogawa H, Takamori K and Yamakura F: Importance of tryptophan nitration of carbonic anhydrase III for the morbidity of atopic dermatitis. Free Radical Bio Med *73*: 75-83, 2014.
26 Thiele JJ, Hsieh SN, Briviba K and Sies H: Protein oxidation in human stratum corneum: susceptibility of keratins to oxidation *in vitro* and presence of a keratin oxidation gradient *in vivo*. J Invest Dermatol *113(3)*: 335-339, 1999.
27 Castro JP, Jung T, Grune T and Almeida H: Actin carbonylation: from cell dysfunction to organism disorder. J Proteomics *92*: 171-180, 2013.
28 Castro JP, Ott C, Jung T, Grune T and Almeida H: Carbonylation of the cytoskeletal protein actin leads to aggregate formation. Free Radical Bio Med *53(4)*: 916-925, 2012.
29 Xu XZ, Garcia MV, Li TY, Khor LY, Gajapathy RS, Spittle C, Weed S, Lessin SR and Wu H: Cytoskeleton alterations in melanoma: aberrant expression of cortactin, an actin-binding adapter protein, correlates with melanocytic tumor progression. Modern Pathol *23(2)*: 187-196, 2010.

Received October 10, 2017
Revised November 7, 2017
Accepted November 10, 2017